



International Journal of Heavy Vehicle Systems

ISSN online: 1741-5152 - ISSN print: 1744-232X
<https://www.inderscience.com/ijhvs>

Optimisation of series electric hybrid wheel loader energy management strategies using dynamic programming

Mohamed Allam, Matti Linjama

DOI: [10.1504/IJHVS.2025.10070996](https://doi.org/10.1504/IJHVS.2025.10070996)

Article History:

Received:	12 November 2024
Last revised:	26 November 2024
Accepted:	14 March 2025
Published online:	13 May 2025

Optimisation of series electric hybrid wheel loader energy management strategies using dynamic programming

Mohamed Allam* and Matti Linjama

Innovative Hydraulics and Automation Lab,
Automation and Engineering Science,
Tampere University,
Tampere, 33720, Finland
Email: mohamed.allam@tuni.fi
Email: matti.Linjama@tuni.fi
*Corresponding author

Abstract: Hybrid non-road mobile machines offer a solution to the low efficiency of diesel-powered machines, but their energy management strategies depend heavily on machine-specific duty cycles. This paper uses experimental data from a 5.7-ton diesel wheel loader performing an industry-standard Y-cycle to optimise and compare four control strategies for fuel savings. Dynamic programming is first applied to determine the optimal power split between the diesel generator and battery. The resulting optimal control sequence is then used to tune thermostat control, power follower control, equivalent consumption minimisation (ECMS), and adaptive equivalent consumption minimisation (A-ECMS) strategies. Simulations in MATLAB Simulink, using both measured Y-cycle data and an artificial half-load cycle, evaluate the performance of each strategy. Results show that A-ECMS achieves fuel consumption within 0.37% of the dynamic programming optimum, followed by thermostat and power follower control. Additionally, different loading conditions influence the relative effectiveness of the management strategies.

Keywords: hybrid machines; non road mobile machines; optimal control; thermostat control; power follower control; dynamic programming; equivalent consumption minimisation; energy storage.

Reference to this paper should be made as follows: Allam, M. and Linjama, M. (2025) 'Optimisation of series electric hybrid wheel loader energy management strategies using dynamic programming', *Int. J. Heavy Vehicle Systems*, Vol. 32, No. 7, pp.1–29.

Biographical notes: Mohamed Allam received his MSc at Ain Shams University, Egypt, in 2020. He is currently working as a Doctoral Researcher at Tampere University, Tampere Finland. He is pursuing a PhD in Automation Science and Engineering. He is currently working in Tampere University's Innovative Hydraulics and Automation Lab. His work is mainly in energy efficient machines, hybrid technologies, power-trains modelling and simulation.

Matti Linjama obtained his D Tech degree at Tampere University of Technology, Finland, in 1998. Currently, he is an Adjunct Professor at the Automation Technology and Mechanical Engineering Unit, Tampere University. He started the study of digital hydraulics in 2000 and has focused on the topicsince then. Currently, he is a Leader of the Digital Hydraulics Research Group,and his professional interests include the study of hydraulic systems with highperformance and energy efficiency.

1 Introduction

Climate change is pushing manufacturers towards new technologies to improve the efficiency of energy consumers in non-road mobile machinery (NRMM). Several approaches to meet the regulations have emerged over the past few decades to power NRMM including battery electric, hybrid electric and hydrogen fuel cells. The latter face the most challenges and are yet to be commercialised as opposed to battery and hybrid power due to the lack of infrastructure to produce and store hydrogen, high production cost and safety concerns. Battery electric are currently widespread in passenger cars and light commercial vehicles to a great extent but when it comes NRMM less battery powered machines are available due the power requirements of such machines, limitation in range and charging infrastructure and weight of the batteries.

Hybrid power-trains provide a solution to these shortcomings where the energy is produced through a diesel engine, no recharging is required, the range of machine operation mainly depends on the fuel available, there are fewer safety concerns and they provide some of the efficiency of battery power. However, this comes at the cost of higher initial cost and more complexity of construction and control. The complexity arises due to the presence of two energy sources which are chemical and electrical where in order to fully utilise the hybrid power-train's fuel saving potential its energy management strategy must be properly designed and optimised.

The energy management strategies (EMS) of hybrid power-trains are diverse and were reviewed and studied extensively for passenger cars (Tran et al., 2020; Salmasi, 2007; Pisu and Rizzoni, 2007; Shabbir, 2015; Bayindir et al., 2011; Cao et al., 2023) and a little less for NRMM (Zhang et al., 2019; Wang et al., 2016). For passenger cars they can be extended and adapted easily to any type of vehicle due to the availability of standardised driving cycles that facilitate the EMS optimisation and also since passenger cars' sizes and mode of operation is not as diverse as NRMM.

The driving cycles for passenger cars represent a recording of vehicle speed during its phases of operation where the total load required from a vehicle can be calculated using the kinematic relationships imposed by the drive-train. However, this abstraction is not viable for NRMM due to their diversity in size, mode of operation and even functionality. For example, wheel loaders' load may originate from driving, using implement and auxiliaries pumps where the use of these components is not restricted to driving as in passenger cars. Also, the loading conditions vary immensely in terms of mean power and duration where

loaders may work in shifts up to 4 h at a time unlike passenger cars where the driving cycles are shorter. On the other hand, there are some properties that are specific to wheel loaders or NRMM which is repeatability where a machine may perform the exact same task for several hours. Another distinction is the abundance of heavy load transients during operations and the extreme variations of load between minimum and maximum as well as positive and negative.

The diversity of NRMM and their loading conditions pose a challenge for the adaptation and optimisation of EMS where each machine must be separately configured and studied as it utilises a unique operating cycle. There have been some studies to design EMS for different NRMM, for example, Lin et al. (2003) uses dynamic programming (DP) to extract rules for a rule based power management strategy of a parallel hybrid electric truck using the standard UDDSHDV cycle, Wang et al. (2017) uses a rule based management strategy to recuperate energy from an electric operated forklift device, Teodorescu et al. (2017) implements an ECMS supervisory control on the power-train of a HEV forklift truck. For excavators, Zhang et al. (2006) uses a constant work point to control a parallel hybrid system in an excavator while Xiao et al. (2008); Lin et al. (2008) use a dynamic work point for a similar construction excavator also Wang et al. (2011) uses fuzzy logic control for the power-train of a hybrid excavator and fine tunes the parameters of membership functions using genetic algorithm. Another NRMM and the main focus of this paper are series hybrid electric wheel loaders (SHEWL) which have been studied previously, for example, Shafikhani and Aslund (2021) proposes an analytical optimal solution for the EMS by using Pontryagin's minimum principle and the same author studies an MPC-based EMS considering battery life for a series electric hybrid wheel loader (Shafikhani et al., 2021). Also, a systematic comparison of four different control strategies but for a parallel hybrid loader is performed (Zeng et al., 2014).

A common observation for the cited NRMMs control studies is that each machine has a different duty cycle with different power requirements, mean loading and overall varying characteristics introducing the need to study each machine independently and optimise the EMS according to real-world cycle measurements. It is challenging to apply regular EMS of passenger cars in a NRMM application. NRMM demand more flexibility, higher power output, and the ability to operate efficiently under widely varying conditions. These machines experience transient and unpredictable loads unlike passenger cars where the power demand is consistent. This variance in loading conditions degrades the efficiency of simple EMS rendering them suboptimal (Vukovic et al., 2017). Additionally, NRMM typically require much higher power output and for a longer duration of operation. For instance, a wheel loader may need to produce higher torque to operate its hydraulic systems while simultaneously maintaining motion. Adapting a passenger car EMS, which is designed for smoother power demands, cannot meet the peak power and energy storage needs in NRMMs. Other special challenges include idle time, NRMM frequently experience extended idle periods, where the engine is running but not actively performing work (Vukovic et al., 2018), followed by sudden transient loads. Traditional EMS strategies for passenger cars focus on optimising fuel economy during more consistent driving cycles and may not adequately handle these periods of low energy demand followed by high consumption adding to the challenges of adapting the EMS. Since the differences above

make it difficult to use duty cycles for passenger cars, experimental measurements from a similar conventional wheel loader were chosen as the basis of calculating the desired load (Allam et al., 2024) during operation of the SHEWL (Linjama et al., 2024).

In this work, a case study for a 5.7 ton SHEWL that is currently under construction in Tampere University IHA Lab is presented, where the experimental measurements are utilised to optimise and compare four different EMS for the SHEWL. This is done to study their fuel saving ability using real world data and incorporating commercially available components for the constructed machine. Firstly, a DP algorithm is used to define the optimum trajectory of the battery's state of charge (SOC) which in turn defines the power split between the two energy sources and the minimum fuel consumption achievable using the selected components. Then, results from DP are used to compare and optimise four control strategies which are

- 1 thermostat control
- 2 power follower control
- 3 equivalent consumption minimisation
- 4 adaptive equivalent consumption minimisation.

Furthermore, the EMS are simulated in a MATLAB Simulink model using full load Y-cycle and an artificial half load one representing lower mean load to evaluate their robustness. Additionally, the behaviour of each EMS in terms of battery SOC, power and diesel generator (DEGEN) performance are studied for both loads. Finally, fuel consumption results from each is presented and compared to global optimum from DP algorithm.

The paper is organised as follows: Section 2 presents the SHEWL system architecture, Section 3 demonstrates the modelling of the components while Section 4 illustrates the simulation environment including the developed DP algorithm, details of the studied duty cycle and model flow. Section 5 introduces the studied EMS and their optimisation. Section 6 shows the results of the simulation followed by a discussion in Section 7. Finally, Section 8 provides a conclusion.

2 System architecture

The machine of this study is a 5.7-ton SHEWL where the overall architecture shown in Figure 1. The machine consists of a diesel engine powered electric permanent magnet synchronous generator (PMSG) connected to a high power lithium-ion battery through a DC-bus, the bus then supplies power to four electric motors for the front drive, rear drive, working implements and auxiliaries respectively. The implements and auxiliaries are both operated by fixed displacement pumps. The power flow between each of the electric components is controlled through a central power distribution unit (PDU). The SHEWL will be used as a research platform to study energy efficient hydraulics, thermal management of batteries and electric motors as well as the development of autonomous systems. The constructed machine is shown in Figure 2 and the main components specifications are illustrated in Table 1.

Figure 1 Series electric hybrid wheel loader system architecture (see online version for colours)

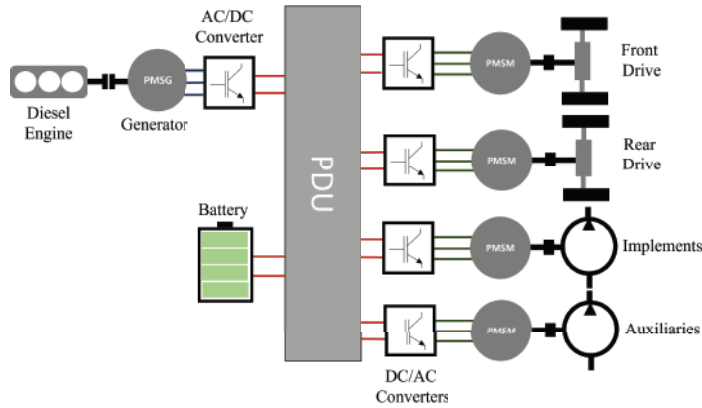
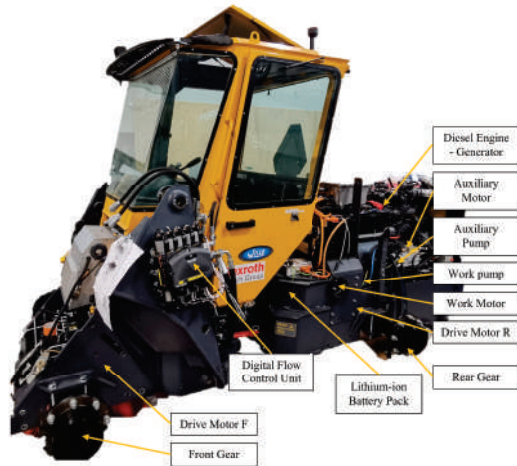


Figure 2 Hybrid wheel loader under construction (see online version for colours)



Source: Allam et al. (2024)

3 Component modelling

In this section the main components of the SHEWL simulation model are described where the modelling of main parts needed for the EMS to work is simplified. The energy management's role is to compute the necessary input based on the load which was calculated in detail previously (Allam et al., 2024) and the current battery's SOC. The simulation model used is an inverse approach where the load that is pre-calculated is followed precisely by system. This guarantees that the results are consistent and are also comparable. The main drawback of the inverse simulation is that it does not account for the limitations of the system components which is taken into consideration in the controller design.

Table 1 SHEWL components' specifications

<i>Component</i>	<i>Value</i>
Machine mass	5.7 ton
Diesel engine power	91 kW
Drive motors power	65 kW
Implement motor power	65 kW
Side motor power	13.9 kW
Generator power	25.3 kW
Battery power	[-58.2 109.2] kW

3.1 Diesel engine

The diesel engine is simulated using an non-linear efficiency map where the efficiency is a function of the engine's rotational speed and torque:

$$\eta_d = f(T_d, \omega_d) \quad (1)$$

and the engine's output mechanical power is defined by:

$$P_m = T_d \omega_d \quad (2)$$

while the fuel consumption is defined using the input power where:

$$P_{in} = \frac{P_m}{\eta_d} \quad (3)$$

$$m_f = \int \frac{P_{in}}{Q_l} \quad (4)$$

and where m_f is the fuel mass consumed in kg , Q_l is the diesel fuel lower heating value. The efficiency map used to calculate the fuel consumption is shown in Figure 3 which is adapted from a previous research (Immonen, 2013) and fitted to the machine's engine using manufacturer data.

The diesel engine's torque is limited using the maximum torque speed curve and is subject to a one time constant to simulate the dynamics of the crankshaft.

3.2 Generator

The generator is a PMSG which is also simulated based on an efficiency map that is adapted from the manufacturers data sheet. The efficiency is plotted against the torque and rotational speed of the electric machine and is shown in Figure 4.

The efficiency is a function of the generator torque and speed represented by:

$$\eta_g = f(T_g, \omega_g) \quad (5)$$

and the mechanical power is calculated from:

$$P_{g_m} = T_g \omega_g \quad (6)$$

while the electrical power from the generator to the battery is calculated through:

$$P_{ge} = P_{gm} \eta_g \tag{7}$$

Finally, the generator’s torque is limited to the maximum torque available at the current rotational speed according to the manufacturer’s data sheet.

Figure 3 Diesel engine efficiency versus torque and speed adapted from Immonen (2013) (see online version for colours)

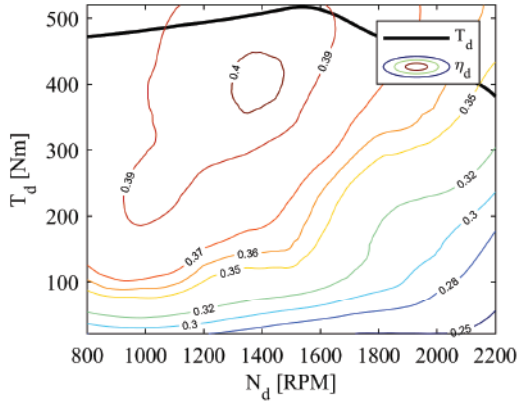
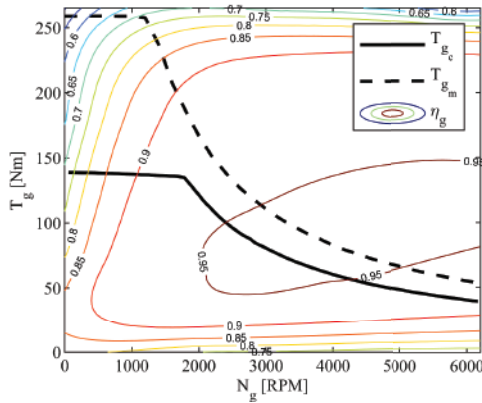


Figure 4 Electric generator efficiency versus torque and speed (see online version for colours)

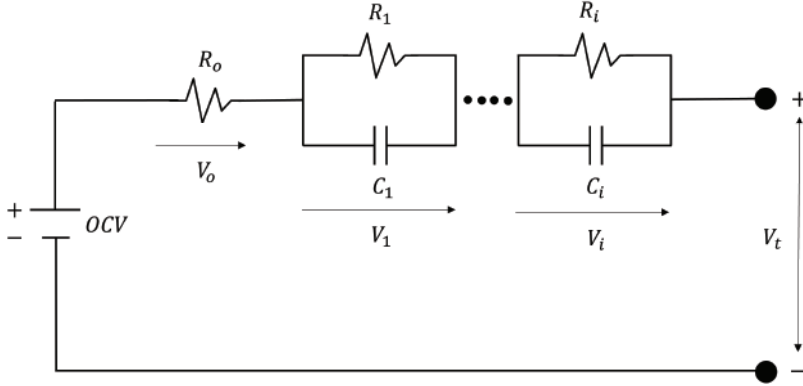


3.3 Battery equivalent circuit model

The dynamics of the battery are described with an equivalent circuit model (ECM) (Plett, 2015) shown in Figure 5 where the model simulates the behaviour of the battery through a series of resistances and resistance-capacitance circuits. The main resistor models the instant dynamics of the battery while the RC circuits represents the slower dynamics of the

diffusion process of lithium. The battery model parameters were estimated using MATLAB parameter estimation toolbox through a pulse discharge test (Jackey et al., 2013). The estimated parameters are a function of the SOC and the relation between the open circuit voltage (OCV) and SOC shown in Figure 6 was adapted from the manufacturer's data sheet.

Figure 5 Lithium-ion battery equivalent circuit model (see online version for colours)



The SOC of the battery is calculated from:

$$SOC(t) = SOC_o - \int \frac{i(\tau)}{3600 \cdot Q} d\tau \cdot \begin{cases} \eta_b & i(\tau) < 0 \\ 1 & i(\tau) > 0 \end{cases} \quad (8)$$

where SOC_o is the initial SOC, Q is the battery's capacity in Ah, η_b is the battery's efficiency and $i(t)$ is the current of the battery calculated from:

$$i(t) = \frac{P_b}{V_t} \quad (9)$$

where V_t is the battery's terminal voltage calculated from the ECM model and P_b is the battery power calculated using:

$$P_b = P_l - P_{ge} \quad (10)$$

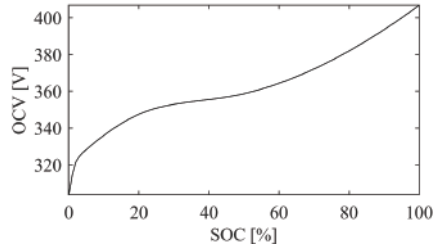
where P_l is the load power and P_{ge} is the generator's electrical power. The estimation of the battery's parameters and the equations used for modelling are detailed in Plett (2015) and Allam et al. (2024). It is worth noting that the model used in the DP algorithm is a simplified Rint model (Plett, 2015) in order to reduce simulation time since the complexity of the model directly affects the calculation time for DP (Sundstrom and Guzzella, 2009; Brahma et al., 2000). Both models provide comparable results for the instant dynamics and the OCV calculation and the main difference is in the slower dynamics of the cell which does not affect the results noticeably (Saldana et al., 2019). The formula for calculating the battery's supply power in DP and A/ECMS is:

$$P_s = OCV \frac{OCV - \sqrt{OCV^2 - 4R_{int}P_b}}{2R_{int}} \quad (11)$$

where OCV is the OCV which is a function of the SOC calculated from (8) and R_{int} is the internal resistance for the DP Rint model is a function of the current direction and SOC where:

$$R_{int} = \begin{cases} R_{ch}(SOC) & i(\tau) < 0 \\ R_{dis}(SOC) & i(\tau) > 0 \end{cases} \quad (12)$$

Figure 6 The relation between the OCV and SOC of the lithium-ion battery pack



4 Simulation environment

The following subsections present the methodology used in this study to compare the different EMS and how DP is formulated. First, DP is introduced as a benchmark optimisation tool, describing its implementation. This is followed by an explanation of the duty cycle measurements and calculations that were used for performance evaluation, based on realistic data from a wheel loader Y-cycle. Details are also provided to illustrate how the fuel consumption is calculated in order to guarantee objectiveness. Finally, the specific constraints imposed by the system components are described.

4.1 Dynamic programming

Dynamic programming (DP) is an optimisation algorithm based on Bellman's principle of optimality which states that each step taken at any time in a system has an effect on the total cost of the problem (Bellman, 2010; Bertsekas, 2020). The DP algorithm requires the evolution of the states to be discrete so that the solution space becomes finite. The discretisation of the states directly affects the optimality of the solution where a finer step will provide better results but at the cost of computation time. Since each step in the decisions of the wheel loader powertrain affects the overall solution i.e., the fuel consumption, the problem can be solved in a backward fashion using DP. However, this means that a duty cycle must be known in advance to find a solution which is not applicable in reality. Therefore, DP is only used as a benchmark in order to optimise and compare the different control strategies investigated. The DP function used in this study is presented in detail in Sundstrom and Guzzella (2009).

In order to reduce the computation time for DP a simpler model for the battery is used. The model also implements the SOC as the one dynamic state variable since the computation

time of DP increases exponentially with the number of states and the DEGEN power as the control variable, where the model can be defined as:

$$SOC(t+1) = f(SOC(t), P_g, P_l) + SOC(t) \quad (13)$$

and the optimisation problem is defined as minimising the fuel consumption of:

$$J = \sum_{k=0}^{N-1} \Delta m_f(P_g, k) \cdot T_s \quad (14)$$

where the input variables are subject to the following constraints:

$$SOC(t_f) = SOC(0) \quad (15)$$

$$P_l(t) = P_b(t) + P_{g_e}(t) \quad (16)$$

$$SOC_l < SOC(t) < SOC_h \quad (17)$$

$$0 < P_g(t) < P_{g_{max}} \quad (18)$$

$$P_{b_{min}} < P_b(t) < P_{b_{max}} \quad (19)$$

$$i_{min} < i(\tau) < i_{max} \quad (20)$$

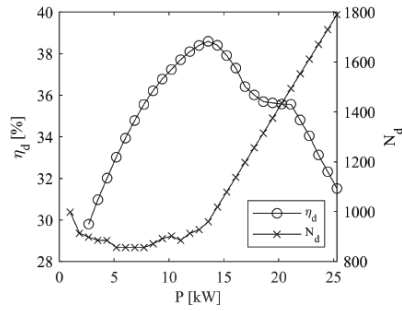
$$\omega_{d_{min}} < \omega_g < \omega_{d_{max}} \quad (21)$$

$$0 < T_g < T_{g_{max}} \quad (22)$$

Since the future driving cycle is known, it is now possible to calculate the cost of each of the possible candidates of the decision variable P_g in a backward fashion. Each grid point from the final time step t_f can be calculated and then stored in an array of costs, and after all the time steps from the end to the beginning are calculated, it is possible to determine the path with the optimal cost; this path will define the optimal power split between the DEGEN and electric power from the battery. The first step is to discretise the decision variable P_g and the state variable SOC . Therefore, SOC is discretised between 0.7 and 0.8 with a step of 0.01 and the DEGEN power is discretised between 0 and $P_{g_{max}}$ with a step of 0.2 kW. The operating point of the DEGEN is selected by tabulating the power output of the DEGEN with rotational speed through the optimum operating line (OOL) and the torque is calculated from the power and rotational speed. The rotational speed versus the output power are shown in Figure 7.

The cost calculated is the fuel consumption from the diesel engine efficiency map as detailed in the modelling section. At each point in time where a power split is selected the value of SOC is calculated according to the governing equations. This determines the trajectory of the machine's battery SOC.

Figure 7 Rotational speed of the DEGEN versus output power (optimum operating curve)



In order to fully illustrate the logic for DP algorithm utilised here Figure 8 shows steps of evaluation.

Figure 8 Flow chart of the applied DP algorithm (see online version for colours)

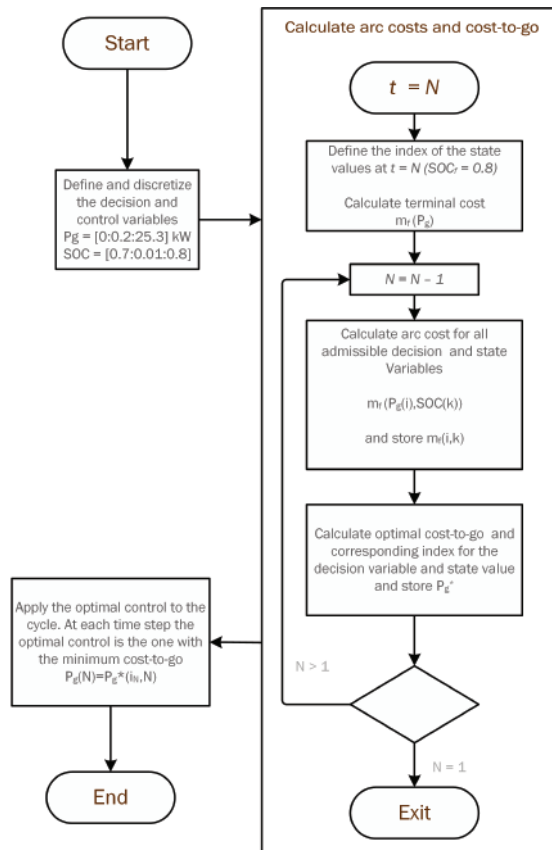
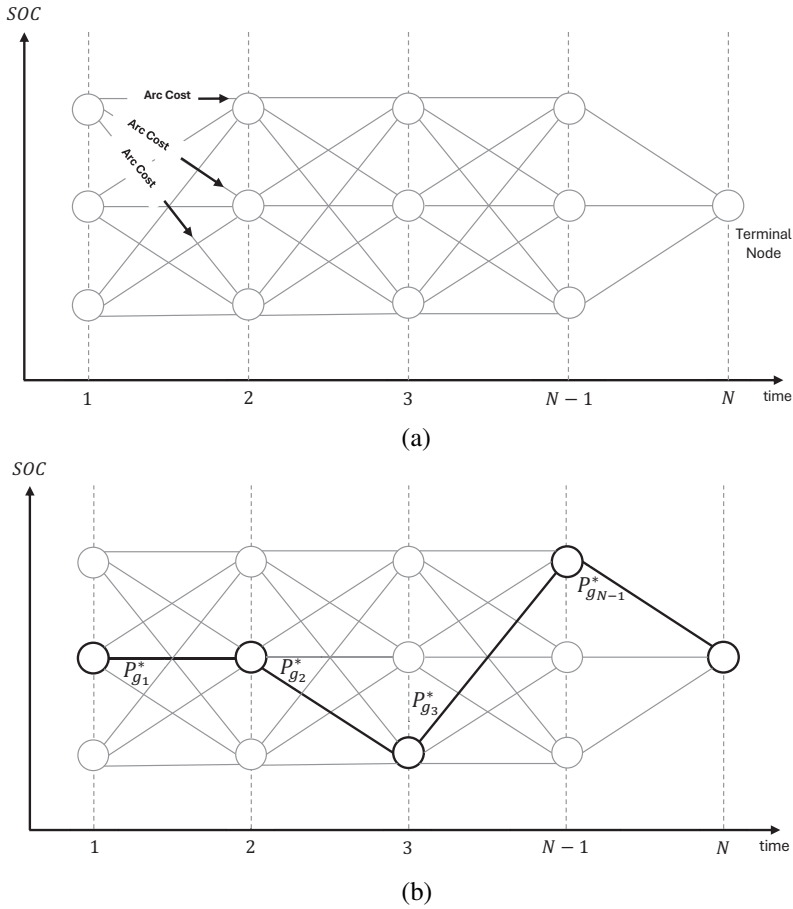


Figure 9 DP algorithm optimisation process: (a) state and decision variables discretisation, arc cost and terminal cost representation of the implemented DP algorithm and (b) optimal decision variable at each time step, minimum cost-to-go and the optimal control sequence for DP



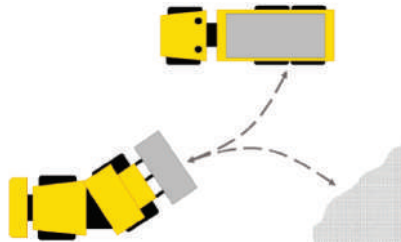
First, the decision and state vectors are defined and discretised then at the final time step t_f all admissible values of the decision variable P_g are used to calculate the terminal cost m_{f_N} where the inadmissible values of the decision variable are set to infinity. In the next steps, as the time goes backwards and at each time step all admissible candidates of the decision variable are then used to calculate the arc cost $m_{f_N}(SOC_N, P_{g_N})$ and stored. The stored values contain the costs of moving from each admissible node at a time step N to the all the admissible values at the next time step $N + 1$. The stored values can be then used to obtain the optimal cost-to-go which is done by selecting the decision variable P_g at each time step which minimises the cost function (fuel consumption). Then, the decision variables which yield the optimum cost are stored in array which represents the optimal progression of decision or in this instance the DEGEN power. Using the optimal progression of the decision variable in a forward manner it is possible to calculate the optimal state sequence SOC .

Figure 9(a) provides an illustration of how the decision variable P_g and the state variable SOC are discretised where each node in the graph represent a state value while the lines connecting the nodes represent the decision variable. Each line is assigned with an arc cost representing the fuel consumption required to move from one node to another (one state to another) and the end point represent the terminal state which is constrained selecting the decision variable that obtains the required final state SOC_f . On the other hand, Figure 9(b) shows the cost-to-go after selecting the minimum cost between each time steps, the thicker black lines have the minimum values for fuel consumption and their corresponding decision variables represent the optimum control at that point, going backwards from the terminal point to the start shows how the optimal control sequence for all the time steps in the control problem.

4.2 Duty cycle

For the purpose of objectively comparing the performance of each controller a realistic driving cycle must be present. The cycle used in this work is the wheel loader Y-cycle (Dadhich et al., 2016) shown in Figure 10. The data of the cycle used was measured experimentally from a conventional diesel powered machine during a Y-cycle loading and unloading gravel where the details of the measurements and calculations are provided in Linjama et al. (2024) and Heikkilä et al. (2018).

Figure 10 The wheel loader short loading cycle used for the simulation (see online version for colours)



Source: Image from Allam et al. (2024)

The Y-cycle was chosen for this study due to the availability of experimental measurements and since it represents the operating conditions of the studied machine quite well. Since the measurements are from a conventional machine they are simulated using a model of the SHEWL in Allam et al. (2024) to calculate the requested load power using the electrical machines and fixed displacement pumps instead of the hydro-static transmission (HST) and variable displacement pumps. The required power from the electric motors of the drive, implements and auxiliaries are shown in Figure 11.

Figure 11(a)–(c) respectively and are used for the calculations in order to gain realistic load information where the total power load profile calculated is presented in Figure 11(d). The negative values represent the machine's capability to recuperate energy through regenerative braking which is equivalent to braking using the HST. It is worth noting that the fluctuation and high power peaks contained in the wheel loader's load differ to a great extent from the passenger cars driving cycles like the WLTP, US06 or NYCC where in these cycles the load may remain steady for longer periods of time and the braking events may

also be longer unlike the wheel loader where during braking there might be a load generated from the implements contributing to a positive overall load. A duration of these cycles is plotted for a conventional passenger car of 1.5 ton in Figure 12 against the Y-Cycle of the wheel loader to highlight the differences.

Figure 11 Y-Cycle data used in the simulation: (a), (b), (c) power required from drive, implements and auxiliaries electric motors respectively and (d) Total power requested by electrical motors calculated in Allam et al. (2024)

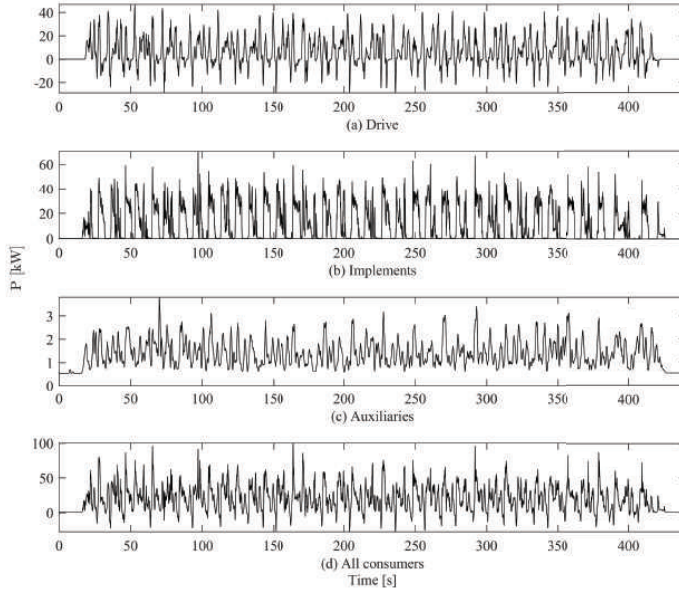
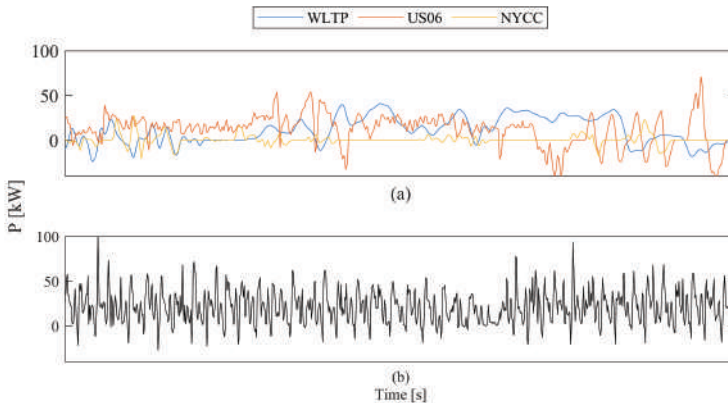


Figure 12 Power requested for: (a) the WLTP, FTP72, NYCC and (b) the Y-Cycle of the wheel loader (see online version for colours)



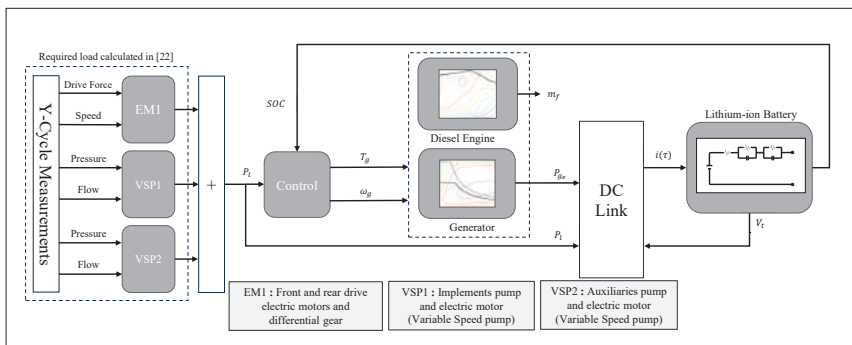
These can affect the optimisation of control strategies, it can also favour one strategy over the other and limit some of the characteristics of some of other control strategies.

In order to evaluate the robustness of the controllers the same load cycle with a lower mean value is simulated which may resemble the same operation but while lifting lighter material instead of gravel. This is done due to the lack of available standardised duty cycles for heavy machinery since they are quite diverse and require the measurement of several phenomenon at the same time and not just the speed of the machine as in passenger cars which was not available to the authors.

4.3 Simulation model

The simulation model is a backward facing one where input from the drive cycle in terms of P_l ; calculated from different consumers; and SOC feedback from the battery are used as input signals to the controller. Each controller then outputs the selected operating points as the DEGEN speed and torque. The diesel engine model is used to calculate the input power required as well as the fuel consumption while the generator model outputs the electrical power P_{ge} using the efficiency map, the electric power from the generator is used in recharging the battery or equalising the load. The DC link calculates the current required from the battery and finally the battery model is used to calculate the terminal voltage and the SOC which is fed back to the controller's. The overall flow of the simulation model is illustrated in Figure 13.

Figure 13 Flow of the simulation model



4.4 Fuel economy evaluation

Electric hybrid architectures pose challenges in terms of fuel consumption evaluation since the system contains two types of energy sources that contribute to the operation of the machine. Namely, the internal combustion engine and the battery where the machine usually depletes the electrical storage device at different stages of the duty cycle making it inaccurate to include only ICE consumption. Therefore, in order to compare different strategies this must be taken into consideration where several approaches are available. One approach is to only consider the consumption of the diesel engine under the assumption that all of the energy eventually comes from the fuel. Nonetheless, under certain operating conditions such as short loading cycles it is possible to power the entire machine using purely electrical energy which would yield zero fuel consumption and the results would be meaningless. To avoid this, it is possible to simulate hours of iterations of the cycle which would render the

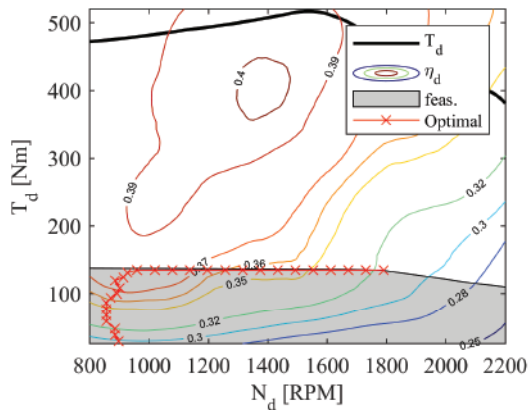
SOC variation negligible and fuel consumption result would be meaningful. However, this would require much longer computation time. Another method is to define a correlation between the chemical and electrical energies where the consumed electrical energy is converted to fuel consumption (Sciarretta et al., 2004; Katrašnik, 2010). Unfortunately, The equivalency factor heavily depends on duty cycle which may be easy to calculate in case of passenger cars where the cycles are well studied and defined, that is not the case with heavy duty equipment and at the same time fuel consumption correction depends on the type of controller itself also making the results unreliable. One final example and the one used here, is to enforce a charge sustaining (CS) constraint where the initial and final SOC are equal meaning that all the energy consumed is from the ICE and zero charge is consumed from the electrical source (Delprat et al., 2004; Musardo et al., 2005; Steinmauer and Del Re, 2001). Hence, the fuel consumption can be measured and compared. It is worth noting that applying this constraint poses some challenges for the optimisation of the control strategies but this is discussed in each controller's section.

4.5 Components specifications

Another challenge in optimisation of different controllers is posed by the component sizing of the constructed machine. For example, the power of the generator is limited compared to the diesel engine which forces the diesel engine to operate in a less favourable region in terms of efficiency. Also, the battery power is higher than the power deliverable by the DEGEN which affects the design and optimisation of the thermostat control strategy where the DEGEN should be able to assist the battery during an extreme loading condition but is unable to do so due to smaller power available.

The constraints above limit the search space of available operating points for the DEGEN where Figure 14 shows the efficiency map of the diesel engine with the optimum efficiency line plotted in red as well as the constraint of the generator torque where the area in grey is the feasible operating area. The OOL represents the torque and speed operating points that achieve the highest possible efficiency at a constant power level. The OOL extends to the maximum efficiency point but this is not the case here due to the component limitation.

Figure 14 Optimal operating curve plotted in red, feasible operating area in grey plotted over the diesel engine efficiency map (see online version for colours)



5 Controllers

The controllers implemented are presented in this section where the goal is to output the operating point of the DEGEN in terms of torque and rotational speed, minimise fuel consumption, respect the machine's physical constraints and achieve a CS strategy. The latter is done by keeping the final SOC as close to the initial SOC as possible in order to properly compare fuel consumption between the different controllers. For each controller, the logic of the operation is presented as well as how their parameters were optimised or selected, how the drawbacks of the CS constraint is mitigated and how the components limitations affect them.

5.1 Thermostat control strategy (TCS)

The thermostat control strategy (TCS) operates as a rule based strategy where the DEGEN mode is selected based on a set of predefined rules (Anderson and Pettit, 1995; Hochgraf et al., 1996; Jalil et al., 1997). The rules depend on the loading condition and the SOC of the battery. Due to the fact that the DEGEN is decoupled from load fluctuations in a series hybrid machine it is possible to operate It freely where the operation point can be selected to be at the most efficient region of the set. The TCS in this work operates according to the following equation:

$$P_g = \begin{cases} 0 & SOC(t) > SOC_h \\ P_o & SOC(t) < SOC_l \\ P_g^- & SOC_l < SOC(t) < SOC_h \end{cases} \quad (23)$$

where $SOC_{h,l}$ are the upper and lower thresholds for mode switching, P_o is a selected DEGEN operation power reference and P_g^- means the generator stays at the previous state of operation until the conditions change. TCS relies mainly on the SOC feedback where the DEGEN is switched on If the SOC is lower than the lower SOC threshold and is left to operate at P_o until the SOC has reached the upper threshold where It is then switched off. In contrary to previous work in passenger vehicles where the DEGEN can when the requested load is more than the battery's power, in this work the battery acts as a power equaliser according to equation (10) and the DEGEN is mostly used for lower power operation as well as recharging as It has limited power when compared to the load request which can reach higher values.

The OOL is used to choose the operating rotational speed and torque which defines P_o . The maximum efficiency of the DEGEN is at 1000 RPM. However, this is not enough to provide a CS system at the end of the studied cycle. Therefore, the wheel loader is simulated at different speeds and the best consumption is at 1600 RPM. To ensure that the selected operating point achieves the least possible consumption given the constraints, results from each simulation run is compared to the global minimum achieved from DP.

It is worth noting that due to the generator limitations the selection of P_o now relies strongly on the properties of the duty cycle as a lower mean power cycle would dictate that the optimum point would be closer to the best operating point to save fuel but at the same time If the machine operates in a demanding cycle the battery may reach dangerous SOC levels.

5.2 Power follower control strategy (PFCS)

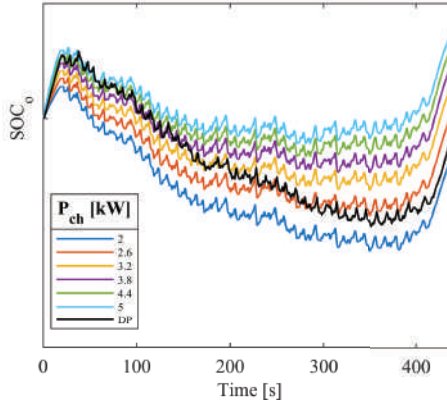
Power follower control strategy (PFCS) operates in a similar fashion to the TCS in terms of defining the operation using a set of rules (Gao et al., 2009; Wang et al., 2007; He et al., 2008). Generally, in PFCS the DEGEN follows the required load profile at all times except for when SOC is higher than the upper threshold or during regeneration. However, in this work the DEGEN follows the required load profile only up to its maximum deliverable power and the rest is supplied by the battery. Here, the battery also acts as an equaliser and PFCS operates according to:

$$P_{gen} = \begin{cases} P_{idle} & SOC(t) > SOC_h \text{ or } P_f < 0 \\ P_f & SOC_l < SOC(t) < SOC_h \\ P_{gmax} & SOC(t) < SOC_l \text{ or } P_f > P_{th} \end{cases} \quad (24)$$

$$P_f = P_l + P_c(SOC_{ref} - SOC(t)) \quad (25)$$

where P_{idle} is the idling power required to keep the DEGEN running, P_f is the power required to follow the load by the DEGEN, P_{gmax} is the maximum power of the DEGEN, P_c is a CS factor for the strategy which can be tuned, SOC_{ref} is the reference SOC which is set to the same value as the initial SOC to keep the strategy as CS and P_{th} is another unable parameter that triggers the DEGEN maximum mode.

Figure 15 SOC of the SHEWL battery using different values of the charge factor P_{ch} plotted with the global optimum from DP (see online version for colours)



The operation of PFCS depends on the load and SOC as inputs where when the SOC is between the upper and lower thresholds the DEGEN will be load following. The DEGEN will idle during regeneration or when the SOC is higher than the higher SOC threshold. Finally, The DEGEN enters maximum mode when the load is more than the predefined load threshold or when the SOC is lower than the lower SOC threshold. The selected P_f is then transformed to operating points in terms of torque and rotational speed using the OOL defined previously.

In order to select P_{ch} and SOC_{ref} the model was simulated for different values of the coefficients and the fuel consumption was compared for all while maintaining a CS

operation in all simulations. Coefficients that yield the best fuel economy are selected. Results from the chosen coefficients are then used to run the simulation and their results are compared to the global optimum produced through DP. Figure 15 shows the SOC of the battery using different values of $P_{ch} = [2 - 5]$ kW where it can be seen that values around 2.6 kW and 3.2 kW yield the closest behaviour when compared to the global optimum.

5.3 Adaptive/Equivalent consumption minimisation strategy (A/ECMS)

The ECMS is a strategy that minimises the fuel consumed by the DEGEN under the assumption that energy sourced from the battery at any point must be replenished either by the engine or through means of regeneration (Onori et al., 2016). The key idea behind ECMS is to define an equivalent fuel consumption formula that includes the fuel consumed by the diesel engine as well as the equivalent fuel needed to replenish the battery. The summation of both yields the instantaneous equivalent fuel consumption that requires minimisation, this defines an optimisation problem which is solved instantaneously at each time step using arguments from the energy flow through the power-train. The flow of the ECMS is shown in Figure 16 where for each time step, P_g is used to define a vector of admissible candidate values of the DEGEN power that satisfy the system constraints. These values are then used to calculate the equivalent fuel consumption for each candidate using the diesel engine efficiency map, battery power, CS function and the equivalency factor. The control combination satisfying the conditions and minimising the fuel consumption is selected for that time step as P_{ref} . Finally, the speed and torque of the DEGEN are selected using the optimum operating curve. The equivalent fuel consumption $\dot{m}_{f_{eq}}$ can be calculated from:

$$\dot{m}_{f_{eq}} = \dot{m}_f + \frac{s(t)}{Q_l} P_s(t) p(SOC) \quad (26)$$

where the cost function is defined as:

$$J = \int_{t_0}^{t_f} \dot{m}_{f_{eq}}(P_{ref}) + \epsilon * I(T_d, \omega_d, SOC, P_b, T_g) \quad (27)$$

where the model used to calculate $P_s(t)$ and the constraints are similar to those used in DP, $s(t)$ is the equivalency factor that must be defined and optimised in prior, $p(SOC)$ is a penalty function used for CS and is defined as:

$$p(SOC) = 1 - \left(\frac{SOC(t) - SOC_{ref}}{(SOC_h - SOC_l)/2} \right)^a \quad (28)$$

where a is a factor that defines the aggressiveness of the constraint, I is the in-feasibility matrix calculated from the constraints and ϵ is a weighing factor.

A key element to the success of the ECMS is the proper definition of the equivalence factor $s(t)$ where the selection of a high factor may lead to lower use of electrical energy and a too low factor would risk the CS of the strategy. It is noticeable that this definition also relies on the properties of the studied cycle where under different conditions where the load profile is different, an ECMS with a properly tuned equivalency factor may perform worse or lose its CS properties. To mitigate this effect, the equivalency factor may be updated each time step according to the difference between the current SOC and the reference SOC or as more known as AECMS. The update at each time step is achieved using a PI controller

where the initial equivalency factor is the optimised equivalence factor used in the ECMS. The optimised equivalency factor is selected using the results of the DP algorithm along with a bisection method and a constraint of CS where the adaptive equivalency factor is defined as:

$$s(t) = s_{opt}(t) + k_p \Delta(SOC) + k_i \int_{t_0}^{t_f} \Delta(SOC) d\tau \quad (29)$$

where s_{opt} is the optimised equivalence factor and k_p and k_i are the proportional and integral gains of the PI controller which were also tuned to find the lowest consumption. To find S_{opt} , the simulation model was run using different values of S_{opt} in the range [1:0.1:5], and the resulting fuel consumption was plotted against the equivalency factor in Figure 17.

Figure 16 A/ECMS Simulink implementation (see online version for colours)

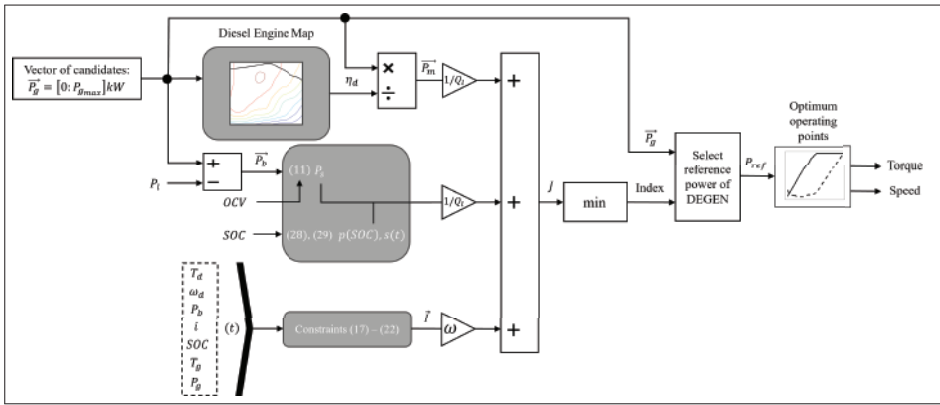
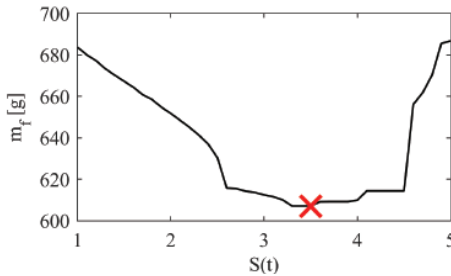


Figure 17 SHEWL fuel consumption versus different equivalency factors using the equivalent consumption minimisation strategy (see online version for colours)

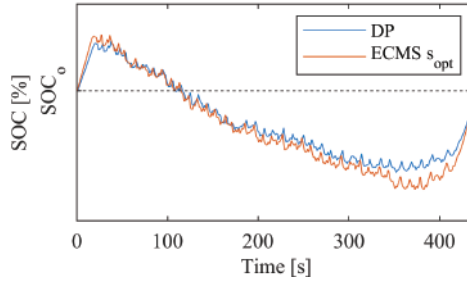


Results show that minimum fuel consumption occurs at around $S_{opt} = 3.3 \sim 3.5$. However, Its important to note that variations in the equivalency factor can lead to different final SOC, which may affect fuel consumption. For lower equivalency factors that yield lower final SOC, the DEGEN is operated at a point that maintains charge sustenance under load until the initial SOC is reached. On the other hand, with higher equivalency factors, fuel

consumption increases because the DEGEN operates at lower efficiency, which prevents achieving further reduction in consumption.

ECMS using the optimised equivalence factor ($s_{opt} = 3.5$) for a one full load cycle is plotted against the optimum SOC trajectory generated using DP in Figure 18. It can be seen how an optimised factor can match the global minimum where the fuel consumption of both is almost equal which will be discussed below.

Figure 18 Optimal SOC trajectory using DP against the ECMS with optimised equivalency factor (see online version for colours)



6 Results

All controllers were simulated using the mentioned cycle repeated for 1 h to resemble one shift of productivity. This is not strictly enforced in order to achieve charge sustenance meaning that the simulation is stopped when the final SOC is equal to the initial SOC with a buffer in simulation time. The small variation in productivity is taken into consideration by measuring the specific fuel consumption relative to the amount of work done in (g/kW-hr) instead of total fuel consumed in kg. Each controller was simulated using the optimised variables for the regular and half load Y-cycle. The parameters for the simulations are illustrated in Table 2.

Table 2 Parameters for the simulation

Parameter	Simulation		Unit
	Full load	Half load	
Step time		0.002	s
$s(t)$	3.5	2.55	ul
a		3	ul
SOC_h		80	%
SOC_l		60	%
SOC_{ref}		80	%
k_p		3	ul
k_i		0.1	ul

6.1 Full load

The SOC variation of each controller when full load is used is shown in Figure 19 while the power distribution between the DEGEN and battery when the loader is in full load is shown in Figure 20.

Figure 19 SOC variation for different controllers using the full load cycle (see online version for colours)

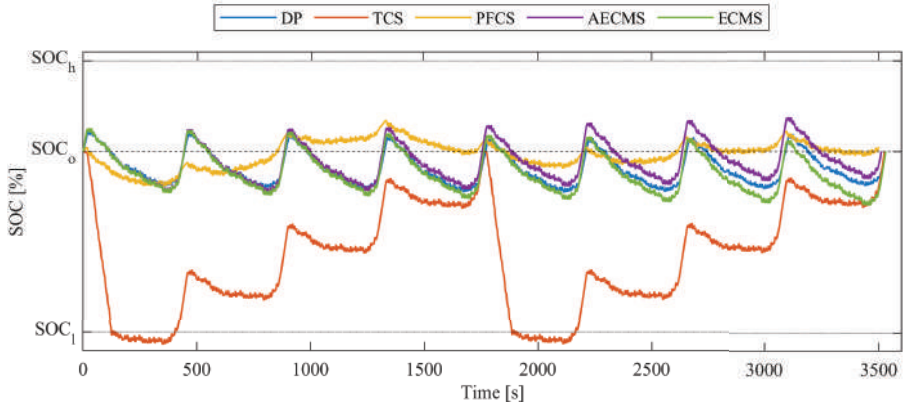
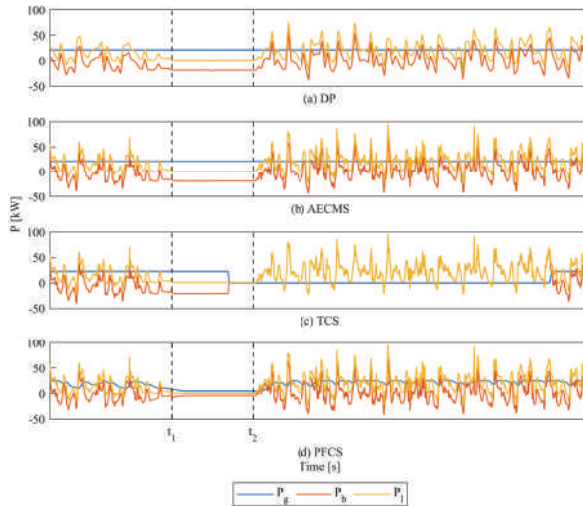


Figure 20 Power distribution between battery and DEGEN for a full load using: (a) DP; (b) AECMS; (c) TCS and (d) PFCS (see online version for colours)



The final SOC of each of the controllers has same value of the initial SOC given the CS constraint with some variations in productivity time. It can be seen that AECMS and ECMS follow the DP trajectory closely for most of the time while PFCS tends to follow the reference SOC rather than the optimum trajectory which means that it is using the DEGEN more

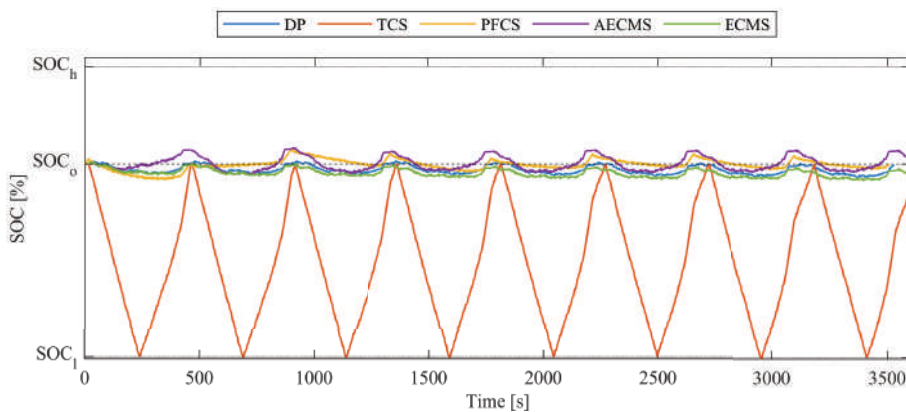
contributing to more fuel consumption. These three strategies restore the battery's SOC to its initial value with small variation from the reference SOC avoiding lower efficiency zones and also maintaining the battery energy level high enough to keep up with the load requirement. On the other hand, TCS behaves as expected where it switches the DEGEN on and off twice during the 1 h operation of the wheel loader reaching the lower threshold during that time.

For the power distribution, AECMS shows similar behaviour to DP algorithm where it uses a constant value for the DEGEN power of 21.17 kW which is the highest possible efficiency achievable while sustaining the charge at the end of the cycle, this value is slightly higher than the mean value of the load studied. Both AECMS and DP use the loader's rest period to recharge the battery while the other strategies follow their respected rules. TCS and PFCS show different characteristics to AECMS where TCS uses the set point of 1600 RPM corresponding to 22.7 kW which is higher than the value used by DP contributing to more fuel consumption and it switches off for the duration where the SOC has reached the higher threshold between t_1 and t_2 where it can be seen that the battery is delivering all the required power, TCS switches the DEGEN on again when the SOC reaches the lower threshold by the end of the shown duration of the cycle. On the other hand, PFCS attempts to follow the load while at the same time keeping the SOC at the reference value, it is noted that PFCS in the beginning of the shown duration of the cycle is in power-follow mode before t_1 while during no load or rest phase between t_1 and t_2 seconds it is in idle mode and after t_2 it switches to power-follow mode again, this time it switches several times to maximum power mode since the SOC is lower than the reference value.

6.2 Half load

The SHEWL is simulated at a half load cycle to test different operating conditions for the controllers, where each controller's tuning parameters were optimised in similar fashion to the full load cycle. The wheel loader's SOC variation for the half load case using different controllers is shown in Figure 21 while the output power is illustrated in Figure 22.

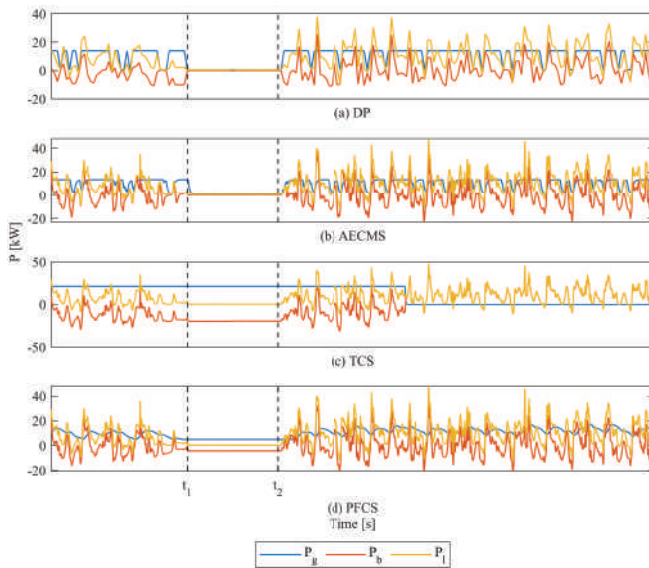
Figure 21 SOC variation for different controllers using the half load cycle (see online version for colours)



It can be seen that the TCS and PFCS show similar behaviour to the full load case where the TCS switches off when the SOC is at SOC_h and switches on when it is at SOC_l , the

switching is more frequently when compared to the full cycle behaviour since the required load is lower and the selected operating point is of higher power. Similarly, PFCS is following the SOC_{ref} with a slightly more aggressive approach due to the lower required load. Conversely, AECMS shows different behaviour compared to the full load cycle case where it deviates from the optimum SOC trajectory produced from DP, this may be attributed to the selection of the a factor or the tuning of $p(SOC)$ parameters. Additionally, the deviation contributes to slightly more fuel consumption when compared to full load operation which will be discussed later. Moreover, ECMS with a properly tuned equivalency factor shows similar behaviour to DP where it follows the closest the optimum SOC trajectory generated by DP. The final SOC for all the controllers is the same as the initial one meaning that the fuel consumption results could be compared.

Figure 22 Power distribution between battery and DEGEN for a half load using: (a) DP; (b) AECMS; (c) TCS and (d) PFCS (see online version for colours)



DP outputs mostly a constant value during the shown portion of the cycle and turns off the DEGEN in regions where the load is very low or during regeneration where the load is negative. AECMS is similar to the DP in terms of the value of output power of the DEGEN where it also uses an equal value for power but with slightly less frequency of idling since switching off the DEGEN is not permitted in the AECMS controller. Additionally, during the period of rest between t_1 and t_2 both DP and AECMS show the same behaviour by using minimum power of the DEGEN. TCS and PFCS again show expected behaviour where TCS switches off once during the shown portion of the cycle as the threshold is reached only once after t_2 and the PFCS is in load following mode for all the selected part except between t_1 and t_2 where it is idling since the load is small and the SOC is close to the SOC_{ref} .

7 Discussion

The fuel consumption of the wheel loader using each of the strategies during full and half loads is illustrated in Table 3. The relative consumption is calculated in comparison to DP. For full load, It can be seen that ECMS achieves the best results followed by the AECMS, TCS and then PFCS. AECMS and ECMS both have close to optimum fuel consumption (+0.16 – 0.37%) as they operate in an identical fashion to DP following the optimal *SOC* trajectory closely. On the contrary, TCS and PFCS both adhere to their respected rules where TCS operates at the selected DEGEN point which contributes to more fuel consumption (+3.74%) while PFCS switches the DEGEN to maximum operating mode more frequently which contributes to the highest fuel consumption (+7.03%). An interesting observation during the half load cycle is that the consumption for the strategies is shuffled. Both AECMS and ECMS achieve the best results when compared to DP since they follow the optimal trajectory the closest but at the same time their overall consumption is higher when compared to full cycle results at (+1.5 – 2%). Similarly, TCS shows higher fuel consumption (+5.15%) since its operating point is selected to achieve CS at all times. On the other hand, PFCS showed improved performance in terms of fuel consumption (+2.45%) as it no longer operates in maximum mode where the results are quite close to the performance of AECMS.

Table 3 Fuel consumption of SHEWL using full load and half load using different strategies

Strategy	Full load		Relative fuel consumption	Half load		Relative fuel consumption
	kg	g/kW-hr	%	kg	g/kW-hr	%
DP	4.891	255.49	–	2.331	243.59	–
AECMS	4.860	256.44	0.37	2.290	248.41	1.98
ECMS	4.854	255.9	0.16	2.345	247.35	1.54
TCS	5.026	265.06	3.74	2.514	256.15	5.15
PFCS	5.051	273.47	7.03	2.367	249.56	2.45

The special operating conditions of NRMMS posed different challenges when configuring each EMS. Commercial components are rarely designed for NRMMS operating conditions which limited the potential of some of the considered EMSs. For example, TCS was not used to its full potential since the generator torque was limited and hence the strategy was not utilised to equalise higher power demands. Also, the tuning of different parameters of PFCS was challenging since the EMS performance varied noticeably with the high variation in the mean load. Similarly, in AECMS, it was difficult to choose a singular equivalency factor that would result in optimal performance in full and half loads. Additionally, this immense variation in loading conditions makes it difficult to have different parameters for various operating cycles since they are not fully standardised or well documented. NRMMS can also operate inconsistently where for times the machine is simply idling and in the next step a transient load needs to be managed which poses a challenge for tuning the AECMS parameters such as the PID gains and the aggressiveness factor α . The parameters could be tuned for half load or full load in the studied case, but in general, they are difficult to tune to a highly different load. For example, in a case where the loader idles more, having parameters that are tuned for higher load could mean that the EMS would try to keep the CS operating the DEGEN more when, in reality, no work is being performed charging the battery needlessly. Finally, the extreme transients abundant in wheel loader's cycles

could mean higher consumption when using PFCS since the diesel engine consumes more fuel when the speed or load are changed more dynamically (Lindgren and Hansson, 2004; Hansson et al., 2003) which is the case when the EMS is attempting to follow the load. In summary, the application of common EMS presents unique challenges when implemented in NRMMs due to their distinct operational characteristics and requirements.

8 Conclusion

This work focused on the study, optimisation and comparison of four distinct EMS for a 5.7 ton SHEWL currently under construction in University IHA lab. The research aimed to evaluate the fuel saving ability of these EMS under realistic loading conditions through the measurement of cycle data of a conventional wheel loader. The measurements included all of the consumers such as the drive, implements and auxiliaries providing accurate representation of the loader operation performing a Y-cycle. The measurements were used in a DP algorithm to define the optimal SOC trajectory, minimum fuel consumption and power split between the two energy sources. DP results were used to optimise the studied EMS, study their behaviour and compare their respected consumption where a 1 h work shift was used to simulate the a typical work shift of the SHEWL. The results showed that AECMS was the most efficient and applicable strategy in all conditions with an average consumption of (+1.2%) more than DP. TCS and PFCS demonstrated similar average consumption (+4.5 and +4.7%) for both loading conditions but higher overall consumption when compared to optimal solution or AECMS. Additionally, the studied strategies performed differently in half load compared to full load. For example, AECMS and TCS showed an increase in fuel consumption while PFCS showed improved performance. In summary, the results highlighted that tailored strategies are essential for varying load conditions and emphasised the need for adaptability in real-world operational scenarios. This study lays the groundwork for further advancements in optimising EMSs for NRMM ;specifically wheel loaders; addressing the adaptations needed for diverse operating conditions which are a key feature for these machines. It also opens the discussion of the issue of component availability for hybrid machine construction commercially, where the components used in the study machine were not tailored specifically for mobile machines but rather selected from a different array of applications which led components to not operate efficiently.

References

- Allam, M., Fernandez, O. and Linjama, M. (2024) 'Fuel efficiency analysis and control of a series electric hybrid compact wheel loader', *SAE International Journal of Commercial Vehicles*, Vol.17, No.02-17-02-0012, pp.197–211.
- Anderson, C. and Pettit, E. (1995) *The Effects of APU Characteristics on the Design of Hybrid Control Strategies for Hybrid Electric Vehicles*, SAE Technical Paper 950493, <https://doi.org/10.4271/950493>.
- Bayindir, K.Ç., Gözüçük, M.A. and Teke, A. (2011) 'A comprehensive overview of hybrid electric vehicle: Powertrain configurations, powertrain control techniques and electronic control units', *Energy Conversion and Management*, Vol. 52, No. 2, pp.1305–1313.
- Bellman, R. (2010) *Dynamic Programming*, Princeton University Press, Princeton.
- Bertsekas, D.P. (2020) *Dynamic Programming and Optimal Control*, Volume 1, Athena Scientific, Belmont, Mass.

- Brahma, A., Guezennec, Y. and Rizzoni, G. (2000) 'Optimal energy management in series hybrid electric vehicles', *Proceedings of the 2000 American Control Conference. ACC (IEEE Cat. No.00CH36334)*, IEEE, Vol. 1, pp.60–64.
- Cao, Y., Yao, M. and Sun, X. (2023) 'An overview of modelling and energy management strategies for hybrid electric vehicles', *Applied Sciences MDPI*, Vol. 13, No. 10, p.5947.
- Lin, C-C., Peng, H., Grizzle, J. and Kang, J-M. (2003) 'Power management strategy for a parallel hybrid electric truck', *IEEE Transactions on Control Systems Technology*, Vol. 11, No. 6, pp.839–849.
- Dadhich, S., Bodin, U. and Andersson, U. Dadhich, S., Bodin, U. and Andersson, U. (2016) 'Key challenges in automation of Earth-moving machines', *Automation in Construction*, Vol. 68, pp.212–222, doi:10.1016/j.autcon.2016.05.009.
- Delprat, S., Lauber, J., Guerra, T. and Rimaux, J. (2004) 'Control of a parallel hybrid powertrain: optimal control', *IEEE Transactions on Vehicular Technology*, Vol. 53, No. 3, pp.872–881, doi:10.1109/tvt.2004.827161.
- Gao, J-P., Zhu, G-M.G., Strangas, E.G. and Sun, F-C. (2009) 'Equivalent fuel consumption optimal control of a series Hybrid Electric Vehicle', *Proceedings of the Institution of Mechanical Engineers, Part D: Journal of Automobile Engineering*, Vol. 223, No. 8, pp.1003–1018, doi:10.1243/09544070jauto1074.
- Hansson, P., Lindgren, M., Nordin, M. and Pettersson, O. (2003) 'A methodology for measuring the effects of transient loads on the fuel efficiency of agricultural tractors', *Applied Engineering in Agriculture*, Vol. 19, No. 3, doi:10.13031/2013.13657.
- He, H-w., Gao, J-p. and Zhang, Y-m. (2008) 'Fuel cell output power-oriented control for a fuel cell hybrid electric vehicle', *2008 American Control Conference*, pp.605–610.
- Heikkilä, M., Huova, M., Tammisto, J., Linjama, M. and Tervonen, J. (2018) 'Fuel efficiency optimization of a baseline wheel loader and its hydraulic hybrid variants using dynamic programming', *BATH/ASME 2018 Symposium on Fluid Power and Motion Control*, doi:10.1115/fpmc2018-8853.
- Hochgraf, C.G., Ryan, M.J. and Wiegman, H.L. (1996) *Engine Control Strategy for a Series Hybrid Electric Vehicle Incorporating Load-Leveling and Computer Controlled Energy Management*, p.960230.
- Immonen, P. (2013) *Energy Efficiency of a Diesel-Electric Mobile Working Machine*, Lappeenranta University of Technology.
- Jackey, R., Saginaw, M., Sanghvi, P., Gazzarri, J., Huria, T. and Ceraolo, M. (2013) *Battery Model Parameter Estimation using a Layered Technique: an Example using a Lithium Iron Phosphate Cell*, SAE Technical Paper Series, doi:10.4271/2013-01-1547.
- Jalil, N., Kheir, N. and Salman, M. (1997) 'A rule-based energy management strategy for a series hybrid vehicle', *Proceedings of the 1997 American Control Conference (Cat. No.97CH36041)*, Vol. 1, pp.689–693.
- Katrašnik, T. (2010) 'Analytical method to evaluate fuel consumption of hybrid electric vehicles at balanced energy content of the electric storage devices', *Applied Energy*, Vol. 87, pp.3330–3339.
- Lin, X., Pan, S-x. and Wang, D-y. (2008) 'Dynamic simulation and optimal control strategy for a parallel hybrid hydraulic excavator', *Journal of Zhejiang University-SCIENCE A*, Vol. 9, No. 5, pp.624–632.
- Lindgren, M. and Hansson, P.A. (2004) 'Effects of transient conditions on exhaust emissions from two non-road diesel engines', *Biosystems Engineering*, Vol. 87, No. 1, pp.57–66.
- Linjama, M., Huova, M., Tammisto, J., Tervonen, J. and Ahola, V. (2024) *6-Ton Wheel Loader Short Y-Cycle Data for 440 Seconds Loading of Gravel*, Zenodo, <https://doi.org/10.5281/zenodo.10639199>

- Musardo, C., Rizzoni, G., Guezennec, Y. and Staccia, B. (2005) 'A-ECMS: an adaptive algorithm for hybrid electric vehicle energy management', *European Journal of Control*, Vol. 11, No. 4, pp.509–524.
- Onori, S., Serrao, L. and Rizzoni, G. (2016) *Hybrid Electric Vehicles*, SpringerBriefs in Electrical and Computer Engineering, Springer London.
- Pisu, P. and Rizzoni, G. (2007) 'A comparative study of supervisory control strategies for hybrid electric vehicles', *IEEE Transactions on Control Systems Technology*, Vol. 15, No. 3, pp.506–518.
- Plett, G.L. (2015) *Battery Management Systems: Volume 1, Battery Modeling*, Artech House Publishers, London.
- Salda na, G., San Martín, J.I., Zamora, I., Asensio, F.J. and O nederra, O. (2019) 'Analysis of the current electric battery models for electric vehicle simulation', *Energies*, Vol. 12, No. 14, p.2750.
- Salmasi, F.R. (2007) 'Control strategies for hybrid electric vehicles: evolution, classification, comparison, and future trends', *IEEE Transactions on Vehicular Technology*, Vol. 56, No. 5, pp.2393–2404.
- Sciarretta, A., Back, M. and Guzzella, L. (2004) 'Optimal control of parallel hybrid electric vehicles', *IEEE Transactions on Control Systems Technology*, Vol. 12, No. 3, pp.352–363.
- Shabbir, W. and Evangelou, S. (2015) *Control Strategies for series Hybrid Electric Vehicles, Control Strategies for Series Hybrid Electric Vehicles*, Thesis, Imperial College London.
- Shafikhani, I. and Aslund, J. (2021) 'Analytical Solution to equivalent consumption minimization strategy for series hybrid electric vehicles', *IEEE Transactions on Vehicular Technology*, Vol. 70, No. 3, pp.2124–2137.
- Shafikhani, I., Sundstrom, C., Aslund, J. and Frisk, E. (2021) 'MPC-based energy management system design for a series HEV with battery life optimization', *2021 European Control Conference (ECC)*, IEEE, Delft, Netherlands, pp.2591–2596.
- Steinmuer, G. and Del Re, L. (2001) 'Optimal control of dual power sources', *Proceedings of the 2001 IEEE International Conference on Control Applications (CCA'01) (Cat. No.01CH37204)*, pp.422–427.
- Sundstrom, O. and Guzzella, L. (2009) 'A generic dynamic programming Matlab function', *2009 IEEE International Conference on Control Applications*, IEEE, St. Petersburg, Russia, pp.1625–1630.
- Theodorescu, C.S., Vandenplas, S., Depraetere, B., Shariatmadar, K., Vyncke, T., Dufflou, J. and Nowe, A. (2017) 'An ECMS-based powertrain control of a parallel hybrid electric forklift', *2017 21st International Conference on System Theory, Control and Computing (ICSTCC)*, IEEE, Sinaia, Romania, pp.763–770.
- Tran, D-D., Vafaiepour, M., El Baghdadi, M., Barrero, R., Van Mierlo, J. and Hegazy, O. (2020) 'Thorough state-of-the-art analysis of electric and hybrid vehicle powertrains: Topologies and integrated energy management strategies', *Renewable and Sustainable Energy Reviews*, Vol. 119, p.109596.
- Vukovic, M., Leifeld, R. and Murrenhoff, H. (2017) 'Reducing fuel consumption in hydraulic excavators: a comprehensive analysis', *Energies*, Vol. 10, No. 5, p.687.
- Vukovic, M., Schmitz, J. and Zhou, J. (2018) *Systematic Data Analysis for Optimal System Design*, [Mainz], <https://doi.org/10.18154/RWTH-2018-224623>
- Wang, D., Lin, X. and Zhang, Y. (2011) 'Fuzzy logic control for a parallel hybrid hydraulic excavator using genetic algorithm', *Automation in Construction*, Vol. 20, No. 5, pp.581–587.
- Wang, J., Yang, Z., Liu, S., Zhang, Q. and Han, Y. (2016) 'A comprehensive overview of hybrid construction machinery', *Advances in Mechanical Engineering*, Vol. 8, No. 3, p.1687814016636809.
- Wang, L., Zhao, D., Wang, Y., Wang, L., Li, Y., Du, M. and Chen, H. (2017) 'Energy management strategy development of a forklift with electric lifting device', *Energy*, Vol. 128, pp.435–446.

- Wang, Z., Li, W. and Xu, Y. (2007) 'A novel power control strategy of series hybrid electric vehicle', *2007 IEEE/RSJ International Conference on Intelligent Robots and Systems*, San Diego, CA, pp.96–102.
- Xiao, Q., Wang, Q. and Zhang, Y. (2008) 'Control strategies of power system in hybrid hydraulic excavator', *Automation in Construction*, Vol. 17, No. 4, pp.361–367.
- Zeng, X., Yang, N., Peng, Y., Zhang, Y. and Wang, J. (2014) 'Research on energy saving control strategy of parallel hybrid loader', *Automation in Construction*, Vol. 38, pp.100–108.
- Zhang, W., Wang, J., Du, S., Ma, H., Zhao, W. and Li, H. (2019) 'Energy management strategies for hybrid construction machinery: evolution, classification, comparison and future trends', *Energies*, Vol. 12, No. 10, p.2024.
- Zhang, Y., Wang, Q., Xiao, Q. and Fu, Q. (2006) 'Constant work-point control for parallel hybrid system with capacitor accumulator in hydraulic excavator', *Chinese Journal of Mechanical Engineering*, Vol. 19, No. 4, pp.505–508.